International Journal of Mathematical, Engineering and Management Sciences
Vol. 8, No. 5, 850-868, 2023
https://doi.org/10.33889/IJMEMS.2023.8.5.049

Design and Analysis of Novel Microstrip-Based Dual-Band Compact Terahertz Antenna for Bioinformatics and Healthcare Applications

Sandeep Kumar
Department of Electronics and Communication Engineering,
School of Engineering and Technology, Maharishi University of Information Technology, Lucknow, India.
Email: sandeepmishra12086@gmail.com

Akhilendra Pratap Singh
Department of Electronics and Communication Engineering,
School of Engineering and Technology, Maharishi University of Information Technology, Lucknow, India.
E-mail: akhilendrasingh.muit@gmail.com

Ashutosh Mishra
School of Integrated Technology, Yonsei University, South Korea.
&
Department of Electronics & Communication Engineering,
Graphic Era Deemed to be University, Dehradun, 248002, Uttarakhand, India.
Corresponding author: ashutoshmishra@yonsei.ac.kr

(Received on June 5, 2023; Accepted on July 11, 2023)

Abstract
This paper presents a compact microstrip-based dual-band antenna for terahertz (THz) technology, catering to the increasing demand for high-frequency, high-gain, and wideband THz antennas. THz technology has numerous applications, including its demands in bioinformatics and healthcare. To address this need, the proposed antenna operates in two frequency bands: 3.6 THz to 4.3 THz and 5 THz to 5.7 THz, enabling its use in THz band communication. The antenna design features a microstrip patch with two transverse slots and one longitudinal slot as a radiator, fed with a microstrip line. The transverse slots enable dual-band resonance, while the longitudinal slots enhance bandwidth and efficiency. Using a 10μm thick polyamide material with a dielectric constant of 3.55, the antenna achieves a compact size of 40 × 40 μm^2, lightweight construction, high radiation efficiency, and a wide impedance bandwidth. Simulation results confirm good impedance matching characteristics, with minimal voltage standing wave ratio and return loss of -10dB or less. The antenna exhibits an impedance bandwidth of -10dB at 700 GHz, a peak radiation efficiency of 85%, a peak gain of 7.86 dB, and an omnidirectional radiation pattern. These favorable attributes position the proposed antenna as an excellent choice for various THz applications, particularly in bioinformatics and healthcare applications.

Keywords- Bioinformatics, Dual-band, Healthcare decision support systems, Microstrip, Terahertz antenna.

1. Introduction

The demand for modern wireless communication systems has driven the need for high data rates, high spectral efficiency, and strong fading mitigation over a wide band. In order to address these requirements, researchers from academia and industry have turned their attention to the unallocated Terahertz (THz) frequency band, ranging from 0.1 to 10 THz (Koenig et al., 2013). This frequency range offers several advantages, including high data speed, low transmission power requirements, and minimal interference (Koenig et al., 2013; Naftaly et al., 2005; Nishizawa et al., 2005; Son, 2009; Woolard et al., 2005). Apart from wireless communication, Terahertz technology has also found applications in healthcare, bioinformatics, remote sensing, environmental monitoring, and extraction of biological information (Galoda & Singh, 2007; Grade et al., 2007; Kumar et al., 2006; Mickan & Zhang, 2003). In the realm of wireless communication, various THz antennas have been developed to cater to different application scenarios. These antennas include horn antennas, substrate-integrated waveguide antennas, microstrip antennas, and more (Alharbi et al., 2017; Bie & Pu, 2021; Dong et al., 2016; Formanek et al., 2009; Gonzalez et al., 2017; Goyal & Vishwakarma, 2018; Guo et al., 2014; Han et al., 2010; Jha & Singh, 2010a; Jha & Singh, 2009; Jha & Singh, 2010b; Jha & Singh, 2012; Kaur et al., 2017; Khamaisi et al., 2013; Kushwaha et al., 2018; Mak et al., 2017; Naghdehforushha & Moradi, 2018a; Naghdehforushha & Moradi, 2018b; Pant & Malviya, 2023; Seyedsharbaty & Sadeghzadeh, 2017; Sharma et al., 2009; Sirmaci et al., 2016; Woolard et al., 2007; Wu et al., 2012; Zhang et al., 2021; Zhou et al., 2014). However, with the exception of microstrip antennas, these structures are three-dimensional and not easily integrated into compact devices. Microstrip antennas, on the other hand, have planar structures that are compact, easy to integrate, and cost-effective. However, they often suffer from limitations such as low gain and narrow bandwidth. Existing literature on microstrip structures for the THz frequency spectrum primarily focuses on single-band or narrow-band designs. Only a few structures have been reported that cover dual bands within the terahertz frequency spectrum (Bie & Pu, 2021; Das & Varshney, 2022; Dong et al., 2016; Jha & Singh, 2010a; Jha & Singh, 2010b; Kaur et al., 2017; Zhang et al., 2021).

Some techniques have been proposed to enhance the performance of microstrip antennas in the THz frequency range. In one approach, multilayer substrate structures are used to improve the radiation properties of the antenna (Jha & Singh, 2010b). Another study utilizes graphene for dual polarization and employs TOPAS as an antenna substrate, incorporating a two-layer substrate design to increase bandwidth and radiation efficiency (Zhang et al., 2021). However, these designs introduce complexity to the antenna structure. In another proposal, a microstrip patch antenna with parasitic feed technology generates asymmetric modes to achieve dual resonance but suffers from deteriorated radiation efficiency (Jha & Singh, 2009). Yet another approach involves a multilayer graphene-loaded patch antenna, which enhances radiation properties but complicates the feeding mechanism (Dong et al., 2016). A multiple split ring patch is also employed to achieve a dual-band patch antenna, but the bandwidth of this antenna is limited (Bie & Pu, 2021). The existing microstrip antenna designs fail to achieve good impedance bandwidth and radiation efficiency for dual bands within the THz frequency spectrum.

In this paper, we present a novel microstrip antenna design that operates with the feature of dual-band frequency ranges of 3.6 THz to 4.3 THz and, 5 THz to 5.7 THz, providing a high gain of approximately 7.86 dB, high radiation efficiency of 85%, and a stable radiation pattern. The motivation for this antenna design comes from the importance of Vitamin K in blood coagulation. Vitamin K exists in two main forms: menaquinone (Vitamin K2) and phylloquinone (Vitamin K1). Vitamin K2 is primarily found in fermented and animal foods, while Vitamin K1 (phylloquinone) is abundant in plant foods, particularly leafy greens (Woolard et al., 2007). Terahertz spectroscopy studies have revealed that Vitamin K2 exhibits absorption frequencies within the 3.6 THz to 4.3 THz and 5 THz to 5.7 THz ranges (Han et al., 2010). Therefore, our proposed antenna is specifically designed to resonate within these frequency bands. The distinguishing features of our proposed antenna include its small dimensions of 40×40 μm² and lightweight construction. It is fabricated on a 10 μm thick polyamide material with a dielectric constant of 3.55. These characteristics make it an excellent choice for applications in terahertz detectors operating within high-frequency bands. The compact size and low weight facilitate easy integration into portable devices or wearable technologies, enabling non-invasive monitoring of Vitamin K levels in the human body. Such monitoring systems can be invaluable in healthcare, allowing for real-time analysis and personalized interventions in cases of blood coagulation disorders or nutritional deficiencies.

Beyond healthcare, the proposed antenna can find applications in bioinformatics and biotechnology. Terahertz technology has proven to be highly useful in analyzing biological samples, including DNA, proteins, and cells. The unique terahertz spectral fingerprints of biomolecules enable their identification and characterization, which can aid in disease diagnosis, drug discovery, and biophysical studies. By leveraging the dual-band operation of the antenna, it becomes possible to perform spectroscopic analysis in a broader frequency range, thereby expanding the potential applications of terahertz spectroscopy in the life sciences. Therefore, the utilization of the unallocated Terahertz frequency band has opened up new possibilities for high-speed wireless communication systems, remote sensing, environmental monitoring, and extraction of biological information. While various THz antenna designs have been explored, microstrip antennas offer advantages in terms of compactness and integration. However, existing microstrip antenna designs for the THz frequency range have bandwidth and radiation efficiency limitations. This paper proposes a novel microstrip antenna that operates within dual frequency bands relevant to Vitamin K spectroscopy. The antenna exhibits high gain, radiation efficiency, and a stable radiation pattern. Its compact size and lightweight construction make it well-suited for integration into terahertz detectors for healthcare and bioinformatics applications, allowing for non-invasive monitoring and analysis of biological samples. As the investigation of THz antennas for the high-frequency band is still in its early stages, further research and development in this area hold great promise for unlocking the full potential of terahertz technology across various domains.

The terahertz antennas are designed to operate in the terahertz frequency range, typically defined as 0.1 to 10 THz. These antennas are used in various applications, including terahertz imaging, spectroscopy, communication systems, and scientific research. Slots are essentially openings or gaps in a conductive material that are intentionally introduced into the antenna structure. They can serve several purposes depending on their configuration and placement. Three slots are used for impedance disturbance, enhancing antenna radiation properties. Below are the details:

- *Radiation Enhancement*: The proposed three-slot design enhances the radiation characteristics of the antenna, such as the directivity, gain, or radiation pattern. It increases antenna efficiency and directs the radiated energy in the desired direction.
- *Frequency Tuning*: The tuning of the operating frequency of the antenna is also adjusted in these three slots. By adjusting the dimensions and placement of the slots, the resonant frequency of the antenna can be modified. This is particularly useful when designing antennas for specific frequency bands (i.e., terahertz).
- *Compactness and Size Reduction*: Slots help reduce the size of the antenna structure while maintaining or enhancing its performance. By introducing slots strategically, the overall size and weight of the antenna can be reduced. This is especially important in applications where compact and lightweight antenna designs are required.

Therefore, we have used three slots in our proposed antenna design. Designing an antenna for dual-band operation involves selecting appropriate antenna elements and configuring them to operate efficiently at two different frequency bands. In our proposed antenna design, we have used an impedance-matching technique to disturb the radiator's surface current at the center. It creates an impedance mismatch that results in a dual band.

1.1 Salient Contribution of the Proposed Work

- The proposed antenna design has a compact size of $40 \times 40\ \mu m^2$, is lightweight, and has a high radiation efficiency, with wide impedance bandwidth.
- It achieves good impedance-matching characteristics.
- It has a small voltage standing wave ratio and return loss of less than -10dB.
- The antenna exhibits an impedance bandwidth of -10dB at 700 GHz.

- It has a peak radiation efficiency of 85%.
- Its peak gain is 7.86 dB.
- It represents an omnidirectional radiation pattern.
- These favorable attributes position the proposed antenna as an excellent choice for various THz applications, particularly in bioinformatics and healthcare applications.

The rest of the paper is organized as follows: Section 2 presents the structural details of the antenna, Section 3 discusses the antenna's parametric optimization and the outcomes of simulation results, and Section 4 presents the conclusion.

2. Materials and Methods

The microstrip antenna is a type of antenna commonly used in various applications, including healthcare and bioinformatics. This antenna consists of a substrate cladded with a perfect electric conductor (PEC) on the top and bottom sides, which helps achieve the desired radiation pattern and performance characteristics. The PEC coating is typically created using the sputtering method, which ensures a uniform and precise deposition of the conductive material (Rius, 2008). In the context of healthcare, microstrip antennas find application in medical devices and wireless body area networks (WBANs). WBANs are networks of wearable sensors and devices that monitor vital signs and transmit the data wirelessly for real-time healthcare monitoring. The compact size and low-profile nature of microstrip antennas make them suitable for integration into wearable devices, such as smart garments or patches, enabling seamless and non-invasive monitoring of patients. These antennas can be designed to operate at specific frequencies, such as those used for medical imaging or communication with medical implants, facilitating efficient data transmission and reception. Microstrip antennas play a role in bioinformatics in various genetic analysis techniques and bio-sensing applications. DNA microarrays are a common tool used in genomics research to analyze gene expression levels and identify genetic variations. Microstrip antennas can be integrated into microarray devices, allowing for efficient wireless communication and data transfer between the microarray chip and external equipment. This wireless connectivity simplifies the experimental setup and enables high-throughput data collection.

Furthermore, microstrip antennas are also used in bio-sensing applications, such as biosensors and lab-on-a-chip systems. Biosensors are devices that detect and analyze biological molecules or chemical substances. Microstrip antennas can be incorporated into biosensor platforms to facilitate wireless communication and remote monitoring of the sensing results. This wireless capability enhances the flexibility and scalability of the biosensor system, allowing for real-time monitoring and analysis of biological samples. In both healthcare and bioinformatics, the dimensions and design of the microstrip antenna are crucial factors. The length and width of the patch on the top side and the substrate dimensions play a significant role in determining the antenna's operating frequency and radiation characteristics. By carefully selecting these dimensions and optimizing the design using equations such as (1) to (5) (Pant & Malviya, 2023), it is possible to achieve specific performance requirements, such as desired operating frequency, bandwidth, gain, and radiation pattern. Microstrip antennas find diverse applications in healthcare and bioinformatics. Their compact size, low-profile nature, and wireless capabilities make them well-suited for integration into wearable devices, medical implants, genetic analysis tools, and bio-sensing platforms. By optimizing the design and dimensions of the antenna, it is possible to achieve the desired performance characteristics necessary for efficient data transmission, reception, and remote monitoring in these applications.

In the proposed microstrip antenna, the substrate is cladded with a perfect electric conductor (PEC) on the top and bottom sides. This conductor coating is developed using the sputtering method (Kaur et al., 2017). The top side of the structure contains a patch whose length and width are w_p and l_p. The substrate and bottom side ground have the same dimension. The substrate length is $l_{s,}$ and the width is w_s. A 3-D perspective, including the top and bottom views of the proposed antenna, is shown in Figure 1. The dimension of the antenna has been calculated by using (1) to (5) (Jha & Singh, 2010a).

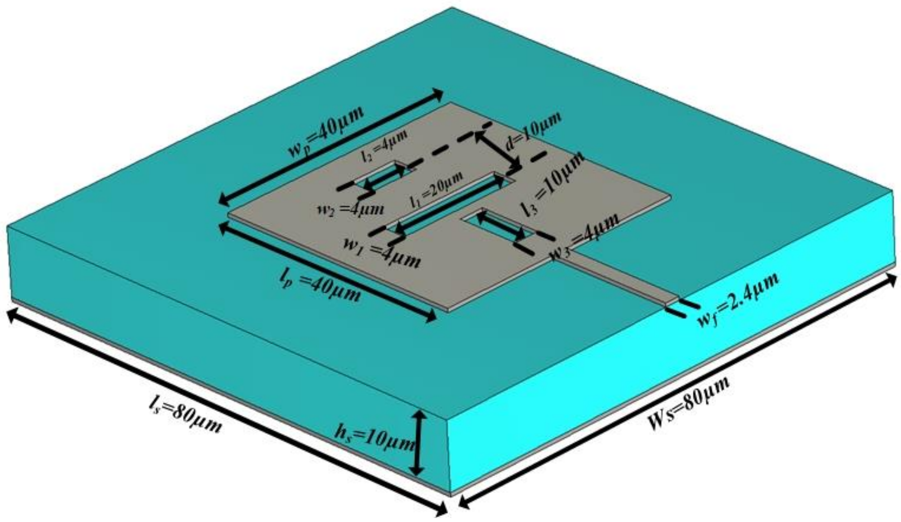

Figure 1. This is the proposed antenna structure.

$$w_p = \frac{1}{2f(\sqrt{\varepsilon_0\mu_0})}\sqrt{\frac{2}{\varepsilon_r+1}} \tag{1}$$

$$l_p = \frac{1}{2f(\sqrt{\varepsilon_{eff}\varepsilon_0\mu_0})} - 2\Delta l_p \tag{2}$$

$$\varepsilon_{eff} = \left(\frac{\varepsilon_r+1}{2}\right) + \left[\left(\frac{\varepsilon_r-1}{2}\right)\left[1+12\frac{h_s}{w_p}\right]^{\left(\frac{-1}{2}\right)}\right] \tag{3}$$

$$l_{eff} = l_p + 2\Delta l_p \tag{4}$$

$$\Delta l_p = 0.412 h_s \frac{(\varepsilon_{eff}+0.3)\left(\frac{w_p}{h_s}+0.264\right)}{(\varepsilon_{eff}-0.258)\left(\frac{w_p}{h_s}+0.8\right)} \tag{5}$$

Here, $\varepsilon_{eff}$is effective permittivity, $\Delta l_p$is an extension in patch length, and l_{eff} is effective patch length. The optimized values of each parameters of the proposed antenna design are tabulated in Table 1. This antenna uses a polyamide substrate with relative permittivity $\varepsilon_r = 3.55$ and a height, h_s which is 10μm. The FDTD-based electromagnetic simulator CST microwave studio is used to design the proposed antenna.

Table 1. Optimized parameters and their values considered in the proposed antenna design.

Parameter	Values(μm)	Parameter	Values(μm)
	80	l_p	40
w_s	80	w_p	40
l_1	20	l_2	4
w_1	4	W_2	4
l_3	10	h_s	10
w_3	4	d	10

3. Results and Discussions

The radiating geometry consists of three evolutions of the microstrip patch, each offering unique characteristics and improvements over its predecessor. The antenna structure is fed by a microstrip feedline, as illustrated in Figure 2. The antenna I serve as the baseline design, featuring a simple microstrip patch with a microstrip feedline. This configuration provides a bandwidth of 3.5 THz, spanning from 3.6 to 5 THz. The antenna operates within this frequency range, effectively radiating signals. Antenna II introduces a significant modification by incorporating a center transverse slot, strategically positioned to disturb the impedance of the antenna. This alteration leads to the creation of a dual-band radiation pattern without compromising the overall radiation performance. The disturbed impedance enables the antenna to operate effectively in two distinct frequency bands, further expanding its potential applications. In the evolution to Antenna III, an additional transverse slot is implemented, positioned 10μm away from the center. This deliberate offset is intended to enhance the radiation efficiency of the antenna. By carefully optimizing the placement and dimensions of the slot using the electromagnetic simulator CST Microwave Studio, the radiation efficiency is significantly improved compared to the previous iterations.

Antenna IV takes another step forward by introducing a longitudinal slot to the design. This slot serves a dual purpose: enhancing the antenna's bandwidth at lower frequencies and perturbing the surface current distribution. By manipulating the surface current, the radiation efficiency is further enhanced, resulting in improved overall performance. The dimensions and placement of the longitudinal slot are optimized using the EM simulator, ensuring the desired effects on impedance and radiation efficiency. Throughout the evolution of the antenna design, careful attention is given to the optimization of slot dimensions and their placement to achieve specific objectives. The electromagnetic simulator, CST Microwave Studio, plays a crucial role in this process, enabling precise analysis and fine-tuning of the antenna parameters. This simulation software allows designers to explore various configurations and evaluate their impact on impedance, radiation efficiency, and bandwidth.

3.1 Surface Current Distribution

The plot of surface current shows the magnitude and phase of the electric current flowing along the surface of the antenna structure. It provides a visual representation of how the current distributes across the antenna surface, revealing areas of high and low current density. By analyzing this plot, antenna designers can gain insights into the efficiency, radiation pattern, and impedance characteristics of the antenna at terahertz frequencies. The surface current plot helps in optimizing the antenna design by allowing engineers to identify potential issues such as current concentrations, discontinuities, or unwanted current paths. It can also aid in the evaluation of different antenna configurations and materials, facilitating the development of antennas with improved performance and desired radiation characteristics in the terahertz frequency range. The perimeter of the current decides the radiation intensity of any antenna.

The resonant frequencies of a dual-band antenna refer to the frequencies at which the antenna exhibits maximum efficiency and performance. Dual-band antennas are designed to operate effectively in two distinct frequency bands. The resonant frequencies are significant because they determine the specific frequency ranges at which the antenna can transmit and receive signals efficiently. The significance of resonant frequencies in a dual-band antenna lies in their ability to match the frequency requirements of different wireless communication systems. By having resonances at two distinct frequencies, the antenna can effectively operate in multiple frequency bands, enabling it to support multiple wireless technologies or communication standards simultaneously.

For example, in the field of mobile communications, a dual-band antenna might be designed to resonate at frequencies commonly used for cellular networks, such as 900 MHz and 1800 MHz or 700 MHz and 2100

MHz. These resonant frequencies correspond to specific frequency bands allocated for cellular communication, and the antenna's ability to efficiently transmit and receive signals at these frequencies ensures reliable wireless connectivity for mobile devices. By utilizing dual-band antennas, wireless devices can take advantage of multiple frequency bands, enabling them to operate in different regions or seamlessly switch between different communication networks. This flexibility in frequency support is particularly useful in areas where various wireless standards or services coexist. It's important to note that the specific resonant frequencies of a dual-band antenna depend on its design, such as the dimensions and configuration of its radiating elements. Antenna engineers carefully design the antenna's structure to achieve optimal performance at the desired frequencies, considering factors like impedance matching, radiation pattern, and bandwidth requirements. Our proposed antenna has resonant frequencies of 3.6 THz and 5.5 THz.

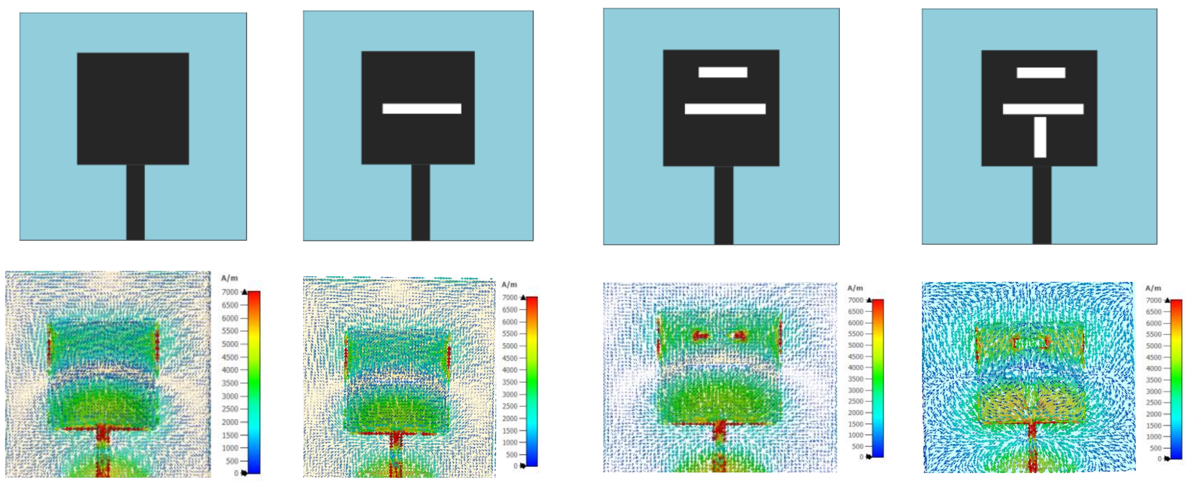

(**a**) (**b**) (**c**) (**d**)

Figure 2. Various antenna development stages with surface current at first resonance frequency at 3.6THZ: (a) Antenna I; (b) Antenna II; (c) Antenna III; (d) Antenna IV.

The iterative improvements in the antenna's design demonstrate the effectiveness of integrating slots into the microstrip patch. By strategically introducing transverse and longitudinal slots, the antenna's performance is enhanced in terms of bandwidth, radiation efficiency, and impedance characteristics. These advancements offer significant benefits for a wide range of applications, including telecommunications, radar systems, and wireless communication. The radiating geometry of the microstrip patch antenna undergoes a series of evolutions, resulting in improved performance with each iteration. The incorporation of transverse and longitudinal slots disrupts the antenna's impedance, enables dual-band operation, enhances radiation efficiency, and expands the bandwidth. Through careful optimization using electromagnetic simulation tools, the dimensions and placement of the slots are fine-tuned to achieve the desired performance characteristics. The evolving antenna design demonstrates the importance of continuous refinement and exploration in antenna engineering, leading to enhanced functionality and versatility in modern wireless communication systems.

The surface current of an antenna is a crucial factor that determines its performance and radiation characteristics. The surface current distribution along the antenna structure plays a significant role in generating and radiating electromagnetic waves at different frequencies. In this context, we have explored the surface current of the antenna at various frequencies, specifically at 3.6 THz, 4.3 THz, 5 THz, and 5.7 THz (as depicted in Figure 3). At 3.6 THz, the antenna's surface current distribution exhibits a specific pattern dictated by the electromagnetic properties of the material and the design of the antenna. The antenna's geometry, dimensions, and electrical properties determine how the current flows on its surface. At this frequency, the surface current is concentrated in specific regions of the antenna, creating areas of high and low current density. These variations in the surface current contribute to the radiation pattern of the antenna and affect its efficiency and directivity. Moving on to 4.3 THz, the surface current distribution of the antenna undergoes changes due to the increase in frequency. As the frequency increases, the electromagnetic waves generated by the antenna have shorter wavelengths, and this affects the current distribution on the antenna's surface. At 4.3 THz, the surface current may exhibit different patterns compared to the previous frequency, resulting in alterations in the radiation characteristics of the antenna.

At 5 THz, the surface current of the antenna experiences further changes. The higher frequency leads to shorter wavelengths, affecting the distribution and magnitude of the surface current. The electromagnetic waves radiated by the antenna at this frequency interact differently with the antenna's structure, influencing the surface current distribution and, consequently, the radiation pattern. It is essential to optimize the antenna design and materials to achieve efficient radiation and minimize losses at this frequency. Finally, at 5.7 THz, the antenna's surface current exhibits yet another pattern due to the increase in frequency. The electromagnetic waves generated by the antenna have even shorter wavelengths at this frequency, resulting in further changes to the current distribution. The surface current may concentrate in specific areas, leading to variations in the radiation properties of the antenna.

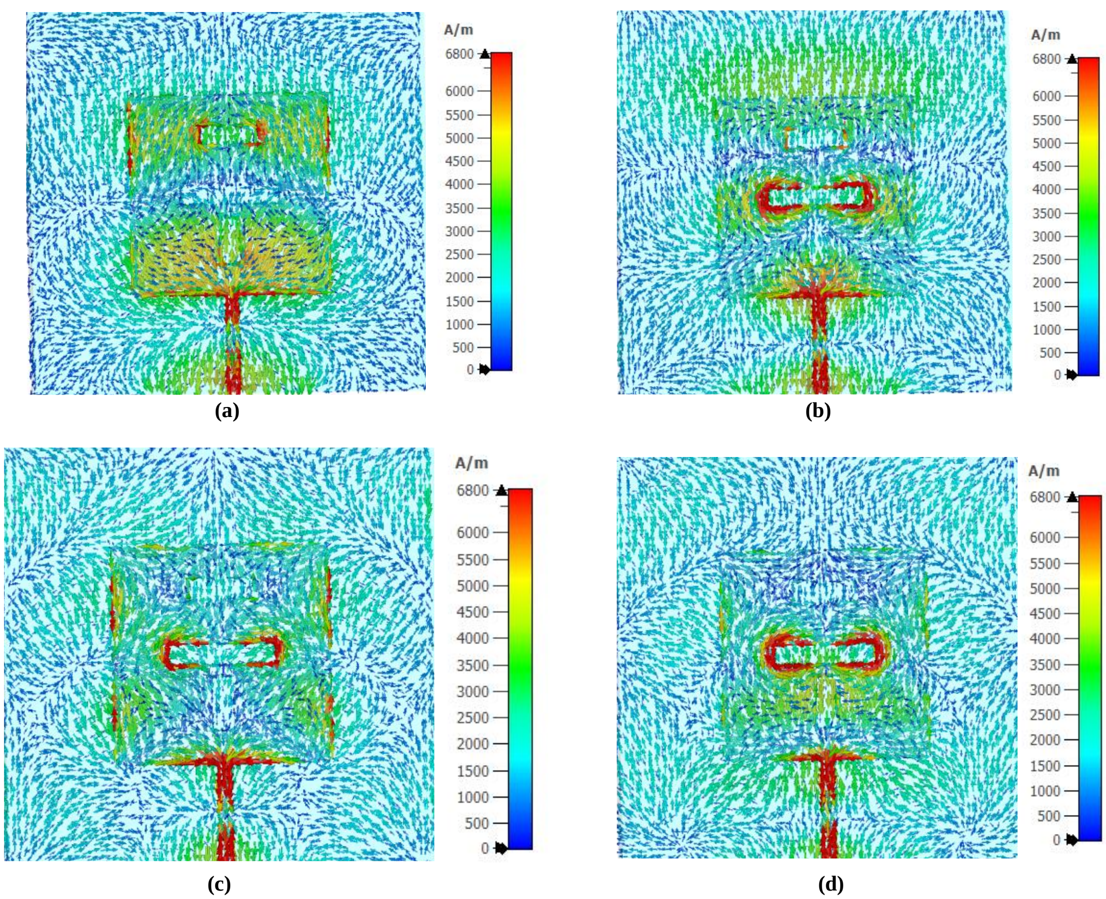

Figure 3. The surface current of the antenna at: (**a**) 3.6 THz; (**b**) 4.3 THz; (**c**) 5 THz; (**d**) 5.7THz.

It is worth noting that the antenna design, material properties, and dimensions play a crucial role in determining the surface current distribution at each frequency. Engineers and researchers employ advanced simulation tools and electromagnetic modeling techniques to analyze and optimize antenna performance at specific frequencies. By studying the surface current distribution, they can fine-tune the antenna's design to achieve desired radiation patterns, gain, and efficiency. The surface current of an antenna varies significantly at different frequencies. The distribution of surface current is influenced by factors such as antenna design, material properties, and electromagnetic wave behavior. As the frequency increases, the surface current distribution changes, impacting the radiation pattern and other performance characteristics of the antenna. Understanding and analyzing the surface current at various frequencies is vital for designing and optimizing antennas for specific applications, such as wireless communication, radar systems, and other wireless technologies.

The proposed three-slot design enhances the radiation characteristics of the antenna, such as the directivity, gain, or radiation pattern. It increases antenna efficiency and directs the radiated energy in the desired direction. From the surface current distribution, we can see different slots participating in radiation at different frequencies. At 3.6 THz smaller slot is participating, while at 4.3 THz, both transverse slots participate. Similarly, at 5 THz center slot is participating, but at 5.7 THz, one transverse and longitudinal slot is participating in radiation.

The gain of an antenna is a crucial parameter that determines its ability to radiate electromagnetic waves efficiently. It is directly influenced by the concentration of surface current on the radiating structure. This relationship between gain and surface current concentration can be observed through the surface current distribution, as depicted in Figure 4. By examining the current flow, one can discern the impact of the mounted slots on the patch, which introduces disturbances in the intensity of the current. In the context of frequency, the participation of transverse slots varies. At lower frequencies, a smaller transverse slot becomes involved, while at higher frequencies, a larger transverse slot comes into play. This implies that the size and positioning of the slots have a direct influence on the behavior of the antenna across different frequency ranges.

3.2 S-Parameter of the Proposed Antenna

To further investigate the performance of the antenna, the s-parameter of the intermediate design antenna step is illustrated in Figure 4.

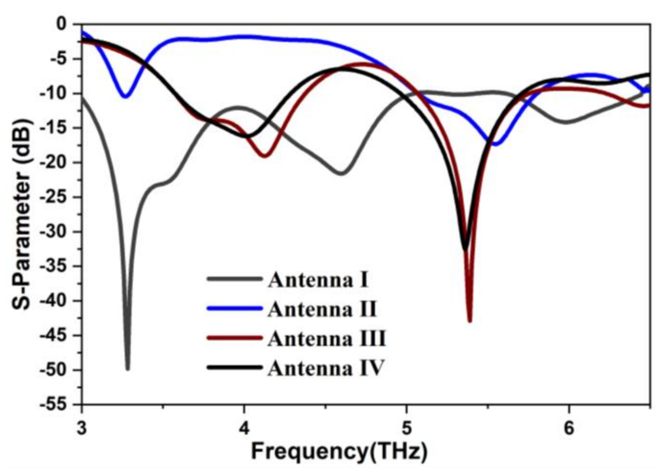

Figure 4. The S-parameter of the proposed antenna.

The s-parameter provides information about the reflection characteristics of the antenna. Looking at Antenna I, it can be observed that the magnitude of reflection remains below -10 dB within the frequency band ranging from 3 to 6.5 THz. This indicates that Antenna I exhibits good reflection properties within this frequency range. Moving on to Antenna II, a transverse slot is mounted, which leads to the separation of the operating band into two distinct frequency bands: 3.5-3.7 THz and 4.9-5.26 THz. The introduction of this slot alters the antenna's response, allowing it to operate in these specific frequency ranges. This demonstrates the ability to customize the antenna's characteristics by incorporating additional structural elements. In Antenna III, yet another transverse slot is added, resulting in surface current perturbations at higher frequencies. This perturbation causes an enhancement in the antenna's bandwidth in the lower frequency band, spanning from 3.56 to 4.4 THz. By carefully manipulating the arrangement and dimensions of the slots, it becomes possible to broaden the operational bandwidth of the antenna, thereby increasing its versatility and performance. The observations made from the surface current distribution and the s-parameter analysis highlight the importance of understanding the impact of structural modifications on antenna performance.

By strategically incorporating slots and perturbations, it is possible to tailor the behavior of the antenna to specific frequency ranges and optimize its gain and bandwidth characteristics. These findings are valuable for antenna designers and researchers who seek to develop antennas with improved performance in specific frequency bands. The ability to manipulate the surface current concentration and customize the operating bands opens up possibilities for various applications, ranging from wireless communication systems to radar systems and beyond. The gain of an antenna is intricately linked to the concentration of surface current on its radiating structure. The surface current distribution and the s-parameter analysis provide insights into the antenna's behavior across different frequencies and highlight the impact of mounted slots on its performance. By carefully designing and incorporating these slots, it is possible to enhance the antenna's bandwidth and optimize its operation in specific frequency bands. These findings contribute to advancing antenna design and pave the way for developing improved and customized antenna systems for a wide range of applications.

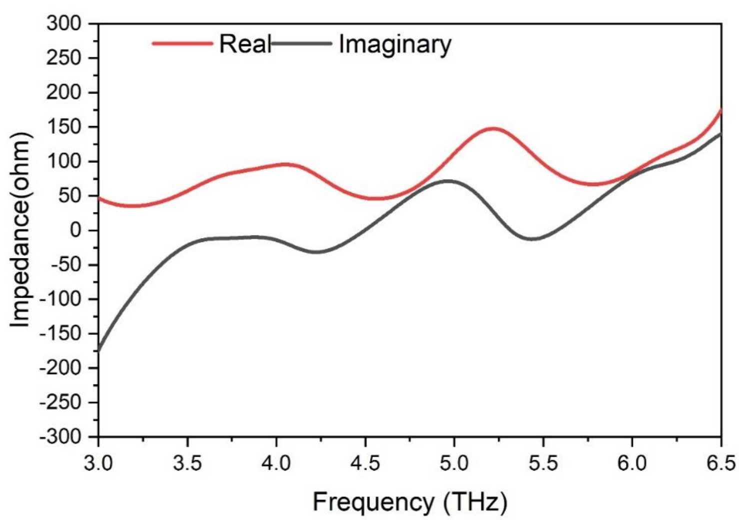

Figure 5. The impedance plot of the proposed antenna.

Antenna IV is designed to increase its bandwidth, and one of the techniques employed to achieve this is incorporating a longitudinal slot. This addition plays a crucial role in enhancing the overall performance of the antenna. Integrating the longitudinal slot significantly expands the antenna's bandwidth, allowing it to operate within a broader frequency range. The bandwidth of Antenna IV is divided into two main bands: the lower and the higher. The resonant frequencies of the antenna are 3.6 THZ and 5.4 THz. In the lower band, the antenna's frequency coverage extends from 3.6 to 4.3 THz, providing an extensive range for transmitting and receiving signals. This expanded bandwidth facilitates the antenna's ability to capture and process a wider range of frequencies, making it more versatile and adaptable to various communication requirements. Similarly, in the higher band, Antenna IV operates within the frequency range of 5 to 5.7 THz. This upper band further extends the antenna's capability to accommodate higher-frequency signals, allowing it to support applications that demand a broader range of transmission and reception. By encompassing both lower and higher frequency bands, the antenna becomes capable of catering to a diverse set of communication needs, ranging from traditional data transfer to advanced wireless applications. To better understand the behavior of the proposed antenna, Figure 5 illustrates the impedance characteristics of the antenna. The impedance graph provides valuable insights into the antenna's performance and its compatibility with the surrounding circuitry. In this case, the graph showcases the real and imaginary parts of the antenna's impedance.

Analyzing the impedance graph, it is evident that the real part of the impedance closely approximates 50 Ω. This value signifies a desirable impedance match between the antenna and the transmission line, ensuring efficient power transfer and minimizing signal reflections. A close match to the standard 50 Ω impedance is advantageous as it allows for seamless integration of the antenna with other components of the communication system, reducing losses and optimizing overall performance.

Furthermore, the imaginary part of the antenna's impedance is observed to be approximately 0 Ω. This characteristic indicates that the antenna's reactive component is minimized or negligible, implying that the antenna is predominantly resistive. A purely resistive impedance simplifies the matching network design and reduces the complexity of impedance matching techniques required for optimal signal transmission. It streamlines the integration process and enhances the overall efficiency of the antenna system. Antenna IV incorporates a longitudinal slot to enhance its bandwidth, enabling it to operate across a wider frequency range. The lower band spans from 3.6 to 4.3 THz, while the higher band covers 5 to 5.7 THz. The impedance characteristics of the proposed antenna demonstrate a close approximation of 50 Ω for the real part and approximately 0 Ω for the imaginary part. These impedance values indicate a favorable impedance match and a primarily resistive behavior, respectively, which are advantageous for efficient signal transmission and integration within communication systems. Antenna IV's extended bandwidth and impedance characteristics make it a valuable tool for a variety of communication applications, catering to diverse needs in the ever-evolving wireless landscape.

Parametric studies of the S-parameter, specifically in relation to slot length and their separation, have been conducted to analyze the behavior of the antenna. The results of these studies are presented in Figure 6. In Figure 6 (a), the variation of the slot length for Antenna II is depicted. It can be observed that as the slot length changes, the resonance frequency of the antenna also varies. This indicates that the slot length plays a crucial role in determining the resonant behavior of Antenna II. By adjusting the slot length, it is possible to tune the antenna to operate at different frequencies within a certain range.

Figure 6 (b) illustrates the impact of lengths l_2 and l_3 on the antenna's performance. Unlike the slot length, variations in l_2 and l_3 do not significantly affect the resonant frequency of the antenna. However, they do have an influence on other important parameters such as bandwidth and reflection coefficient. Adjusting lengths l_2 and l_3 can lead to changes in the antenna's bandwidth, which determines the range of frequencies over which the antenna can operate effectively. Furthermore, modifications in these lengths can also affect the reflection coefficient, which measures the efficiency of power transfer between the antenna and the transmission line.

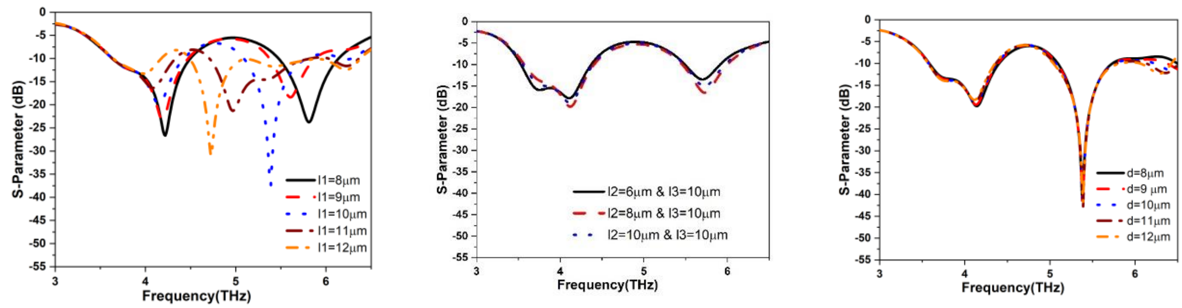

(a) (b) (c)

Figure 6. Parametric studies: (**a**) Slot length, l_1 variation; (**b**) Slot lengths, l_2 & $l_3$variation; (**c**) Separation between l_2 & l_3.

Finally, the study in Figure 6 (c) focuses on the separation between slots in Antenna III. This parameter is optimized to enhance the bandwidth of the antenna. The bandwidth of an antenna is a critical factor as it determines the range of frequencies over which the antenna can efficiently transmit or receive signals. By strategically adjusting the separation between slots in Antenna III, it is possible to achieve a wider bandwidth, allowing for improved performance across a broader frequency range. These parametric studies highlight the importance of slot length and separation in antenna design. By manipulating these parameters, engineers and researchers can tailor the performance characteristics of the antenna to meet specific requirements. The ability to adjust the resonance frequency, bandwidth, and reflection coefficient enables optimization for different applications and frequency bands. This flexibility is valuable in diverse fields, including wireless communications, radar systems, and satellite communications, where antennas with varying specifications may be required. The parametric studies illustrated in Figure 6 demonstrate the significance of slot length and separation in antenna design. By carefully selecting and adjusting these parameters, it is possible to control and optimize the antenna's resonance frequency, bandwidth, and reflection coefficient. These findings contribute to the advancement of antenna technology and enable the development of more efficient and adaptable antennas for various applications.

4. The Radiation Pattern of the Proposed Antenna

The radiation efficiencies depend on the surface current perturbation of slots. In the proposed structure, lower perimeters have less current perturbation resulting in low radiation efficiencies. Similarly, if the perturbation perimeter is more in the design, increasing radiation efficiencies. Here the radiation efficiency variation of 10% only.

The radiation pattern of an antenna is a crucial characteristic that determines its directionality and coverage in different planes. In the case of the proposed antenna, the radiation pattern in the E-plane (electric field polarization) and H-plane (magnetic field polarization) has been analyzed at various frequencies ranging from 3.6 THz to 5.7 THz, as depicted in Figure 7. The results indicate that the radiation pattern of the antenna is omnidirectional in both planes across the entire frequency range. This means that the antenna radiates energy uniformly in all directions, making it suitable for applications where a broad coverage area is desired. Omnidirectional radiation patterns are often desirable in scenarios such as wireless communication systems, where signals need to be transmitted and received from various directions.

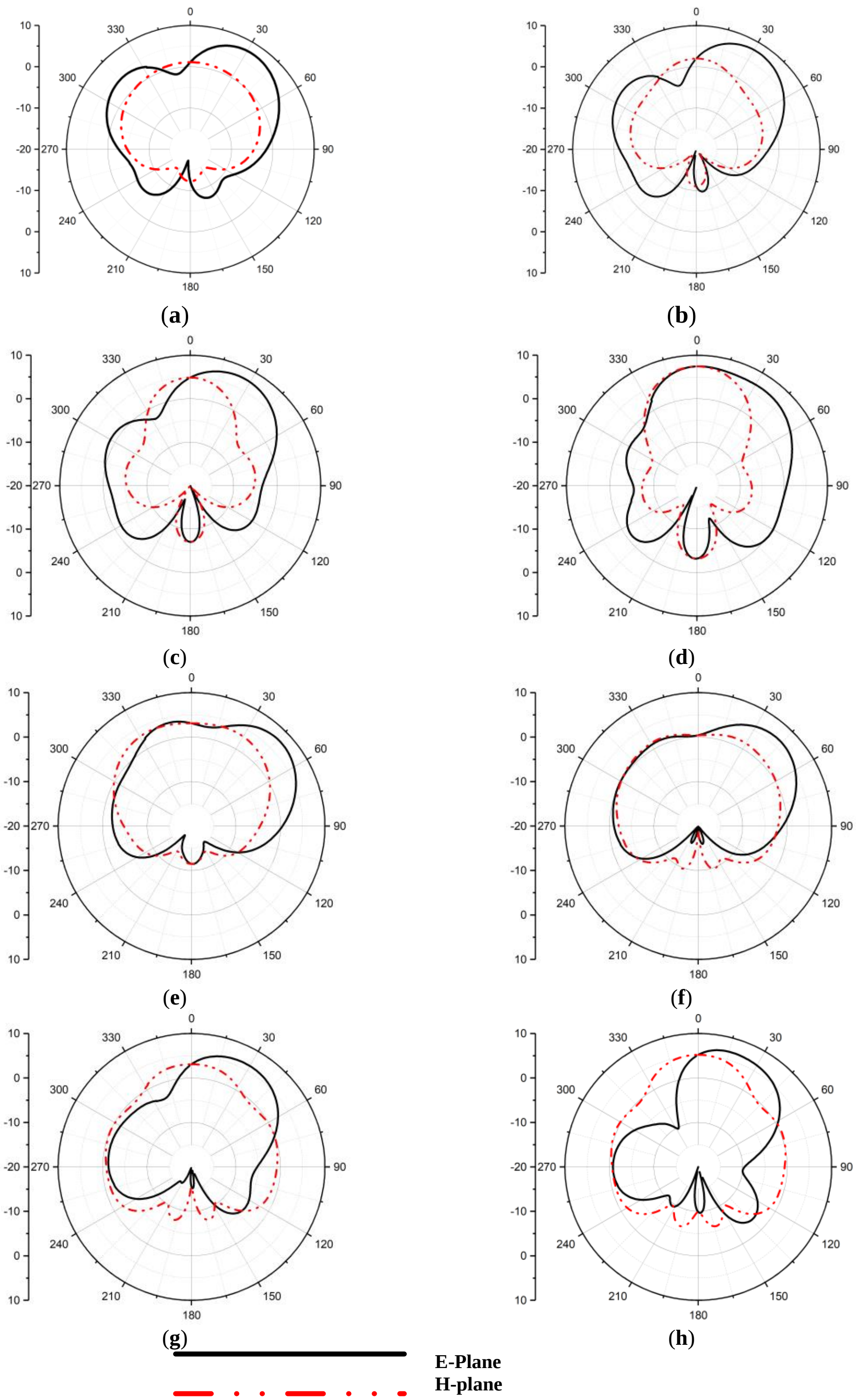

Figure 7. The radiation pattern of: (**a**) 3.6 THz; (**b**) 3.8 THz; (**c**) 4 THz; (**d**) 4.3 THz; (**e**) 5 THz; (**f**) 5.2 THz; (**g**) 5.5 THz; and (**h**) 5.7 THz.

Furthermore, the peak realized gain of the antenna has been measured at each frequency. The gain of an antenna refers to its ability to direct and concentrate energy in a particular direction compared to an isotropic radiator (an ideal, theoretical point source that radiates energy uniformly in all directions). In the first band, which encompasses frequencies from 3.6 THz to 5 THz, the peak realized gain of the antenna varies between 7 dB and 7.86 dB. In the second band, covering frequencies from 5.2 THz to 5.7 THz, the gain ranges from 6.14 dB to 7.5 dB.

5. Radiation Efficiency, VSWR, and Peak Gain

The variation in gain across different frequencies is expected due to the complex interactions between the antenna's structure and the electromagnetic waves at each frequency. These fluctuations in gain can be attributed to factors such as resonance effects, phase differences, and impedance matching. Overall, the analysis of the radiation pattern and gain of the proposed antenna reveals its suitability for omnidirectional coverage, and its ability to provide moderate to high gain across the frequency bands of interest. These characteristics make it a promising candidate for applications requiring wide-angle coverage and efficient energy transfer at frequencies ranging from 3.6 THz to 5.7 THz.

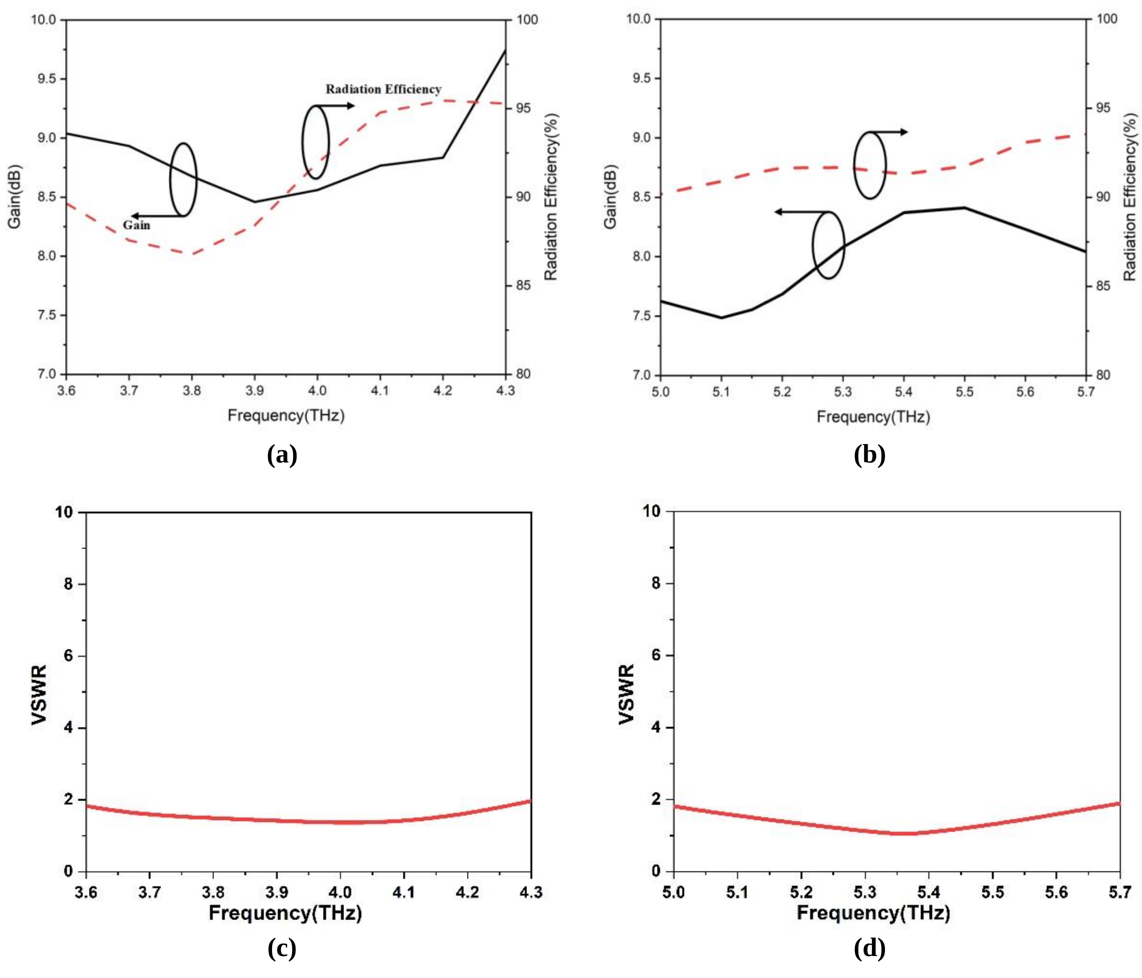

Figure 8. (**a**) Radiation efficiency and gain plot first band 3.6 THz-4.3THz; (**b**) Radiation efficiency and gain plot of second band 5.0 THz-5.7THz; (**c**) VSWR plot of first band 3.6 THz-4.3THz; (**d**) VSWR plot of second band 5.0 THz-5.7THz.

Radiation Efficiency: The radiation efficiency of an antenna refers to the percentage of power that is radiated as electromagnetic waves compared to the total input power. It is influenced by factors such as conductor losses, dielectric losses, and impedance matching. The maximum radiation efficiency is calculated through (6),

$$\text{Radiation Efficiency} = (\text{Radiated Power} / \text{Input Power}) \times 100 \tag{6}$$

Voltage Standing Wave Ratio (VSWR): VSWR is a measure of how well an antenna is impedance-matched to the transmission line feeding it. It represents the ratio of the maximum voltage to the minimum voltage along the transmission line. A low VSWR indicates good impedance matching and efficient power transfer. The VSWR can be calculated using (7),

$$\text{VSWR} = (\text{Vmax}/\ \text{Vmin}) \tag{7}$$

Peak Gain: Peak gain refers to the maximum power gain of an antenna in a specific direction. It quantifies how much the antenna amplifies the input signal in a given direction. The peak gain is obtained by (8), as:

$$\text{Peak Gain} = 4\pi \times (\text{Antenna's Effective Area}) / (\text{Wavelength}^2) \tag{8}$$

Peak radiation efficiency in THz antennas refers to the maximum efficiency with which the antenna converts input electrical power into radiated electromagnetic waves in the terahertz frequency range. It represents the ability of the antenna to efficiently couple and radiate energy at the desired frequency. Radiation efficiency is a measure of how effectively an antenna radiates electromagnetic energy compared to the total power supplied to it. It considers various factors that affect the efficiency of the radiating system, including losses due to resistive elements, impedance matching, and radiation pattern distortions. In the context of terahertz antennas, achieving high radiation efficiency is particularly important due to the unique characteristics of the terahertz frequency range. Terahertz signals are easily attenuated by the atmosphere and other materials, making it crucial to maximize the efficiency of terahertz antennas to compensate for the inherent losses. To optimize peak radiation efficiency in terahertz antennas, various design considerations come into play. These may include selecting suitable antenna materials with low loss properties at terahertz frequencies, optimizing the antenna's geometry and dimensions for efficient radiation, employing proper impedance matching techniques, and minimizing unwanted losses such as conductor and dielectric losses. By maximizing peak radiation efficiency, terahertz antennas can achieve better signal transmission, reception, and overall system performance in terahertz applications. We have used optimizing the antenna's geometry and dimensions for efficient radiation, employing proper impedance matching techniques, and minimizing unwanted losses such as conductor and dielectric losses in our proposed antenna design.

In Figure 8, the radiation efficiency and voltage standing wave ratio (VSWR) of the antenna are depicted. The graph reveals an interesting trend: as the frequency increases, the radiation efficiency of the antenna rises exponentially. This signifies that the proposed antenna is highly effective at converting input power into radiated energy across a wide range of frequencies. Moreover, the radiation efficiency surpasses 85% in both frequency bands, demonstrating the antenna's remarkable performance. To further evaluate the superiority of the proposed antenna, a comparison with existing works is presented in Table II. The table provides a comprehensive overview of various antennas, including their radiation efficiency in dual-band operation. Among the listed antennas, the proposed design stands out as it exhibits the highest radiation efficiency in both frequency bands.

This significant achievement highlights the proficiency and innovation embedded within the proposed antenna. By optimizing the design and leveraging advanced techniques, the antenna achieves exceptional performance metrics, outperforming previous state-of-the-art solutions. The high radiation efficiency indicates that a large portion of the input power is effectively radiated, resulting in improved signal transmission and reception capabilities. The implications of this breakthrough are substantial. The proposed antenna's superior radiation efficiency ensures enhanced wireless communication performance, including increased signal strength, improved data transfer rates, and an extended communication range. These benefits are particularly valuable in applications that rely on dual-band operation, where reliable and efficient signal propagation is essential.

Table 2. Performance assessment with existing works.

References	Size of antenna (μm^2)	No. of Band	Frequency Range (THz)	Bandwidth	VSWR	Maximum gain (dB)	Efficiency (%)
Naghdehforushha & Moradi (2018)	-	Single	0.52-0.56	0.04THz	-	4.5	44
(Kushwaha et al., 2018)	156×168	Single	0.615-0.651	0.036 THz	1.01	7.94	85.7
Naghdehforushha & Moradi (2018a)	133×92.35	Single	0.64-0.82	0.18 THz	1.024	0.7	20
Jha & Singh (2010b)	103×22	Dual	0.7-1.02	0.32 THz	1.2	0.778	30
			2.43-2.67	0.24 THz	2.1		
Dong et al. (2016)	25×25	Dual	4.0-4.8	0.8 THz	1.41	7.2	60
			6.5-7.5	1.0 THz	2.1		
Bie & Pu (2021)	667×544	Dual	0.2741-0.2956	0.0215	1.75	-	-
			0.3063-0.3134	0.0071	1.41		
Jha & Singh (2009)	500×500	Dual	059-0.610	0.2 THz	2.4	9.57	79.7
			0.79-0.81	0.2THz	2		
Ours	40×40	Dual	3.6-4.3	0.7 THz	1.61	7.86	85
			5.0-5.7	0.7 THz	1.21		

The findings presented in Figure 8 and Table 2 underscore the significance of the proposed antenna design. Its exponential increase in radiation efficiency with frequency, coupled with its remarkable performance compared to existing works, establishes it as a cutting-edge solution in the field of antenna engineering. The research and development of such antennas contribute to advancing wireless communication systems, enabling more efficient and reliable connections in a variety of applications, including telecommunications, IoT devices, and wireless networks.

6. Conclusions

This paper introduces a novel microstrip-based compact dual-band THz antenna with potential applications in various fields, including healthcare and bioinformatics. The antenna design incorporates a patch with three slots to achieve dual-band operation, and extensive optimization of slot length and width has been performed to ensure proper impedance matching. The proposed antenna demonstrates impressive performance characteristics across a frequency range of 3.6-4.3 THz and 5-5.7 THz, covering a bandwidth of 700 GHz. This broad frequency spectrum enables the antenna to operate in two distinct THz bands, making it highly versatile for a range of applications. In the healthcare sector, the use of THz technology holds great promise for non-invasive medical imaging, as THz waves can penetrate through many materials, including clothing and biological tissues, without causing harm. With its dual-band capabilities and efficient radiation characteristics, the proposed antenna can be utilized in THz imaging systems to enhance image resolution and depth penetration. This could aid in detecting and diagnosing various conditions, such as skin cancer, burns, and internal organ abnormalities. Bioinformatics is another field that can benefit from the proposed antenna. THz waves have been employed in spectroscopic analysis to study molecular structures and dynamics. The dual-band nature of the antenna allows for more precise and accurate spectroscopic measurements in the THz frequency range. This can contribute to advancements in drug discovery, protein structure analysis, and understanding biological processes at the molecular level.

Moreover, the antenna's triple slot design introduces perturbations in the surface current, which leads to enhanced radiation intensity. This feature is valuable for wireless communication systems operating in the THz band. The antenna's wide impedance matching performance, low voltage standing wave ratio (VSWR), high radiation efficiency (85%), and peak gain (7.86 dB) make it an excellent candidate for reliable and high-speed data transmission in THz communication networks.

In the future, with the proposed antenna design opens doors for ultra-fast wireless communication, data transfer between electronic devices, and high-capacity wireless networking such as applications involved (Bajracharya et al., 2018, Bajracharya et al., 2020, Bajracharya et al., 2022, Shrestha et al., 2021). Therefore, the proposed microstrip-based compact dual-band THz antenna offers a versatile solution for various applications, particularly in healthcare and bioinformatics. Its ability to operate in two distinct THz bands, along with its efficient radiation characteristics, makes it suitable for non-invasive medical imaging, spectroscopic analysis, and high-speed THz communication systems. The antenna's performance parameters make it an attractive choice for researchers and engineers working in these fields, driving advancements in THz technology and its applications. Further, it opens the scope for the design engineers to fabricate this antenna for various wearable devices and sensors to integrate a reliable and high-speed data transmission in the THz band.

Conflict of Interests

Authors declare no conflict of interests.

Acknowledgements

We are thankful to the CST MICROWAVE STUDIO® simulator.

References

Alharbi, K.H., Khalid, A., Ofiare, A., Wang, J., & Wasige, E. (2017). Diced and grounded broadband bow-tie antenna with tuning stub for resonant tunnelling diode terahertz oscillators. *IET Microwaves, Antennas & Propagation*, *11*(3), 310-316.

Bajracharya, R., Shrestha, R., & Jung, H. (2020). Future is unlicensed: Private 5G unlicensed network for connecting industries of future. *Sensors*, *20*(10), 2774.

Bajracharya, R., Shrestha, R., Ali, R., Musaddiq, A., & Kim, S.W. (2018). LWA in 5G: State-of-the-art architecture, opportunities, and research challenges. *IEEE Communications Magazine*, *56*(10), 134-141.

Bajracharya, R., Shrestha, R., Kim, S., & Jung, H. (2022). 6G NR-U based wireless infrastructure UAV: standardization, opportunities, challenges and future scopes. *IEEE Access*, *10*, 30536-30555.

Bie, S., & Pu, S. (2021). Array design of 300 GHz dual-band microstrip antenna based on dual-surfaced multiple split-ring resonators. *Sensors*, *21*(14), 4912. https://doi.org/10.3390/s21144912.

Das, P., & Varshney, G. (2022). Gain enhancement of dual-band terahertz antenna using reflection-based frequency selective surfaces. *Optical and Quantum Electronics*, *54*(3), 161. https://doi.org/10.1007/s11082-022-03548-4.

Dong, Y., Liu, P., Yu, D., Li, G., & Tao, F. (2016). Dual-band reconfigurable terahertz patch antenna with graphene-stack-based backing cavity. *IEEE Antennas and Wireless Propagation Letters*, *15*, 1541-1544.

Formanek, F., Brun, M.A., Umetsu, T., Omori, S., & Yasuda, A. (2009). Aspheric silicon lenses for terahertz photoconductive antennas. *Applied Physics Letters*, *94*(2), 021113. https://doi.org/10.1063/1.3072357.

Galoda, S., & Singh, G. (2007). Fighting terrorism with terahertz. *IEEE Potentials*, *26*(6), 24-29.

Gonzalez, A., Kaneko, K., Kojima, T., Asayama, S.I., & Uzawa, Y. (2017). Terahertz corrugated horns (1.25--1.57 THz): design, Gaussian modeling, and measurements. *IEEE Transactions on Terahertz Science and Technology*, *7*(1), 42-52.

Goyal, R., & Vishwakarma, D.K. (2018). Design of a graphene-based patch antenna on glass substrate for high-speed terahertz communications. *Microwave and Optical Technology Letters*, *60*(7), 1594-1600.

Grade, J., Haydon, P., & van der Weide, D. (2007). Electronic terahertz antennas and probes for spectroscopic detection and diagnostics. *Proceedings of the IEEE*, *95*(8), 1583-1591.

Guo, L., Huang, F., & Tang, X. (2014). A novel integrated MEMS helix antenna for terahertz applications. *Optik*, *125*(1), 101-103.

Han, K., Nguyen, T.K., Park, I., & Han, H. (2010). Terahertz Yagi-Uda antenna for high input resistance. *Journal of Infrared, Millimeter, and Terahertz Waves*, *31*, 441-454.

Jha, K.R., & Singh, G. (2009). Improved performance analysis of square patch microstrip antenna at terahertz frequency. In *2009 International Conference on Advances in Recent Technologies in Communication and Computing* (pp. 676-679). IEEE. Kottayam, Kerala India.

Jha, K.R., & Singh, G. (2010a). Dual-band rectangular microstrip patch antenna at terahertz frequency for surveillance system. *Journal of Computational Electronics*, *9*, 31-41. https://doi.org/10.1007/s10825-009-0297-8.

Jha, K.R., & Singh, G. (2010b). Analysis and design of rectangular microstrip antenna on two-layer substrate materials at terahertz frequency. *Journal of Computational Electronics*, *9*, 68-78. https://doi.org/10.1007/s10825-010-0306-y.

Jha, K.R., & Singh, G. (2012). Analysis and design of terahertz microstrip antenna on photonic bandgap material. *Journal of Computational Electronics*, *11*, 364-373. https://doi.org/10.1007/s10825-012-0416-9.

Kaur, G., Mehta, V., & Sidhu, E. (2017). Rectangular terahertz microstrip patch antenna design for vitamin K2 detection applications. In *2017 1st International Conference on Electronics, Materials Engineering and Nano-Technology* (pp. 1-3). IEEE. Kolkata, India.

Khamaisi, B., Jameson, S., & Socher, E. (2013). A 210–227 GHz transmitter with integrated on-chip antenna in 90 nm CMOS technology. *IEEE Transactions on Terahertz Science and Technology*, *3*(2), 141-150.

Koenig, S., Lopez-Diaz, D., Antes, J., Boes, F., Henneberger, R., Leuther, A., Tessmann, A., Schmogrow, R., Hillerkuss, D., Palmer, R., Zwick, T., Koos, C., Freude, W., Ambacher, O., Leuthold, J., & Kallfass, I. (2013). Wireless sub-THz communication system with high data rate. *Nature Photonics*, *7*(12), 977-981.

Kumar, P., Singh, A.K., Singh, G., Chakravarty, T., & Bhooshan, S. (2006). Terahertz technology-a new direction. In *Proceedings of IEEE International Symposium on Microwave* (pp. 195-201). Bangalore India.

Kushwaha, R.K., Karuppanan, P., & Malviya, L.D. (2018). Design and analysis of novel microstrip patch antenna on photonic crystal in THz. *Physica B: Condensed Matter*, *545*, 107-112.

Mak, K.M., So, K.K., Lai, H.W., & Luk, K.M. (2017). A magnetoelectric dipole leaky-wave antenna for millimeter-wave application. *IEEE Transactions on Antennas and Propagation*, *65*(12), 6395-6402.

Mickan, S.P., & Zhang, X.C. (2003). Terahertz sensing technology. In Woolard, D.L., Loerop W.R., & Shur, M.S. (eds), *Terahertz Sensing Technology* (pp. 1-35). World Scientific. Singapore.

Naftaly, M., Foulds, A.P., Miles, R.E., & Davies, A.G. (2005). Terahertz transmission spectroscopy of nonpolar materials and relationship with composition and properties. *International Journal of Infrared and Millimeter Waves*, *26*, 55-64. https://doi.org/10.1007/s10762-004-2033-6.

Naghdehforushha, S.A., & Moradi, G. (2018a). Design of plasmonic rectangular ribbon antenna based on graphene for terahertz band communication. *IET Microwaves, Antennas & Propagation*, *12*(5), 804-807.

Naghdehforushha, S.A., & Moradi, G. (2018b). Plasmonic patch antenna based on graphene with tunable terahertz band communications. *Optik*, *158*, 617-622.

Nishizawa, J.I., Sasaki, T., Suto, K., Yamada, T., Tanabe, T., Tanno, T., Sawai, T., & Miura, Y. (2005). THz imaging of nucleobases and cancerous tissue using a GaP THz-wave generator. *Optics Communications*, *244*(1-6), 469-474.

Pant, R., & Malviya, L. (2023). THz antennas design, developments, challenges, and applications: A review. *International Journal of Communication Systems*, *36*(8), e5474.

Rius, G.S. (2008). *Electron lithography for nanofabrication*. Ph.D. Dissertation, Universitat Autonoma de Barcelona, Bellaterra, Spain.

Seyedsharbaty, M.M., & Sadeghzadeh, R.A. (2017). Antenna gain enhancement by using metamaterial radome at THz band with reconfigurable characteristics based on graphene load. *Optical and Quantum Electronics*, *49*, 1-13. https://doi.org/10.1007/s11082-017-1052-1.

Sharma, A., Dwivedi, V.K., & Singh, G. (2009). THz rectangular microstrip patch antenna on multilayered substrate for advance wireless communication systems. In *Progress in Electromagnetics Research Symposium* (pp. 627-631). Beijing, China.

Shrestha, R., Omidkar, A., Roudi, S.A., Abbas, R., & Kim, S. (2021). Machine-learning-enabled intrusion detection system for cellular connected UAV networks. *Electronics*, *10*(13), 1549.

Sirmaci, Y.D., Akin, C.K., & Sabah, C. (2016). Fishnet based metamaterial loaded THz patch antenna. *Optical and Quantum Electronics*, *48*, 1-10. https://doi.org/10.1007/s11082-016-0449-6.

Son, J.H. (2009). Terahertz electromagnetic interactions with biological matter and their applications. *Journal of Applied Physics*, *105*(10), 102033. https://doi.org/10.1063/1.3116140.

Woolard, D.L., Brown, R., Pepper, M., & Kemp, M. (2005). Terahertz frequency sensing and imaging: A time of reckoning future applications?. *Proceedings of the IEEE*, *93*(10), 1722-1743.

Woolard, D.L., Jensen, J.O., & Hwu, R.J. (2007). *Terahertz science and technology for military and security applications* (Vol. 46). World Scientific. Singapore.

Wu, K., Cheng, Y.J., Djerafi, T., & Hong, W. (2012). Substrate-integrated millimeter-wave and terahertz antenna technology. *Proceedings of the IEEE*, *100*(7), 2219-2232.

Zhang, J., Tao, S., Yan, X., Zhang, X., Guo, J., & Wen, Z. (2021). Dual-frequency polarized reconfigurable terahertz antenna based on graphene metasurface and TOPAS. *Micromachines*, *12*(9), 1088. https://doi.org/10.3390/mi12091088.

Zhou, T., Cheng, Z., Zhang, H., Le Berre, M., Militaru, L., & Calmon, F. (2014). Miniaturized tunable terahertz antenna based on graphene. *Microwave and Optical Technology Letters*, *56*(8), 1792-1794.